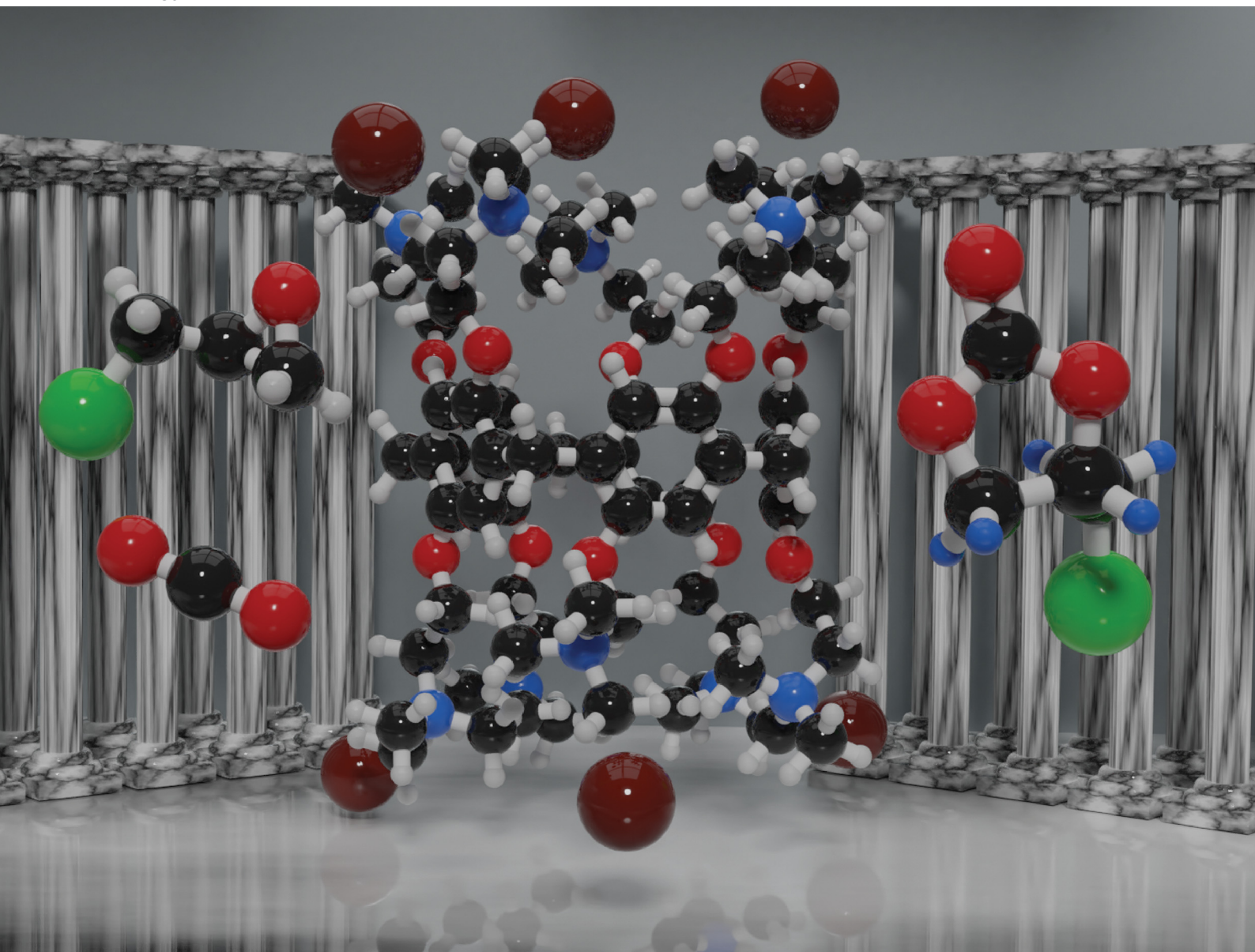


Energy Advances

Volume 4
Number 4
April 2025
Pages 463–590

rsc.li/energy-advances



ISSN 2753-1457

PAPER

Khaleel I. Assaf, Feda'a M. Al-Qaisi *et al.*
An ammonium rich pillararene macrocycle as a
heterogeneous catalyst for cyclic carbonate synthesis

Cite this: *Energy Adv.*, 2025,
4, 530

An ammonium rich pillararene macrocycle as a heterogeneous catalyst for cyclic carbonate synthesis†

Khaleel I. Assaf,^a Feda'a M. Al-Qaisi,^b Ala'a F. Eftaiha,^b
Abdussalam K. Qaroush,^c Ahmad M. Ala'mar^b and Majd M. Al-Farajeh^b

The development of efficient catalysts for the cycloaddition of CO₂ with epoxides to produce cyclic carbonates (CCs) under mild reaction conditions remains a highly attractive research area. This study presents a trimethyl ammonium-rich pillar[5]arene (**N(Me)₃⁺-P5**) macrocycle as a promising heterogeneous catalyst for this reaction. The catalyst design ensures a complementary dual-function mechanism to facilitate the catalytic process. The ammonium groups activate the epoxides, and the bromide ions act as nucleophiles to initiate the ring opening. Optimized reaction conditions using 0.7 mol% catalyst loading and a CO₂ balloon at 80 °C, resulted in high CC yields, particularly with sterically unhindered epoxides. Furthermore, **N(Me)₃⁺-P5** can be reused for at least five catalytic cycles, demonstrating its potential for sustainable applications.

Received 26th December 2024,
Accepted 3rd March 2025

DOI: 10.1039/d4ya00620h

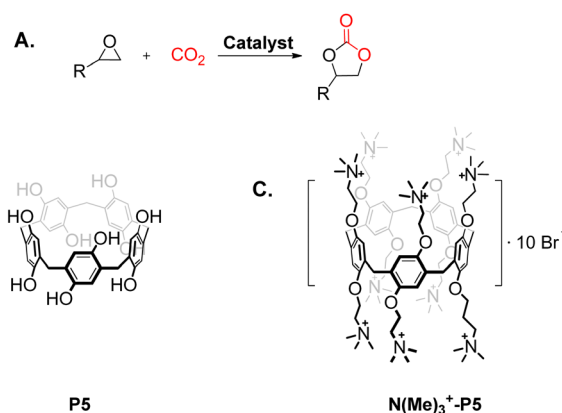
rsc.li/energy-advances

1. Introduction

Developing value-added chemicals from CO₂ presents a significant economic opportunity,^{1–4} enabling the generation of products such as methanol, formic acid, polycarbonates, and cyclic carbonates (CCs). The latter have diverse applications, including their use as green solvents and in lithium-ion batteries.^{5,6} The atom-economical cycloaddition reaction between CO₂ and epoxide to synthesize CCs is a well-established approach (Scheme 1A).^{7–9} Therefore, the development of catalytic systems to improve the efficiency of this reaction has garnered significant attention within the CO₂ research community.⁷ A variety of catalysts have been explored, such as ammonium-based catalysts,^{10,11} ionic liquids (ILs),^{12–14} metal complexes,^{15–17} metal organic frameworks (MOFs),^{18,19} covalent organic frameworks (COFs),²⁰ and porous organic polymers (POPs).²¹

Designing catalysts that achieve high catalytic activity under mild and greener conditions, while overcoming the limitations of homogenous catalysts, such as recyclability and demanding product purification, as well as avoiding the use of external additives for cooperative activation,^{22,23} remains a significant

challenge. While numerous organocatalysts have been investigated, the catalytic role of macrocyclic molecules, such as cyclodextrins,²⁴ cucurbiturils,²⁵ calixarenes,²⁶ and pillararenes,²⁷ in the CC formation remains relatively understudied. For instance, pristine β-cyclodextrin (β-CD) has been shown to participate in the catalytic conversion of propylene oxide (PO) to propylene carbonate (PC).²⁸ When used synergically with potassium iodide (2.5 mol%), it resulted in a 98% yield of the CC product within 4 hours under 6 MPa CO₂ pressure and 120 °C. Moreover, onium-functionalized β-CD, incorporating ammonium, imidazolium, or pyridinium groups, has shown high yield and



Scheme 1 (A) Cycloaddition reaction of epoxide with CO₂. (B) and (C) Chemical structure of pillar[5]arene (**P5**) and ammonium-rich pillar[5]arene (**N(Me)₃⁺-P5**), respectively.

^a Department of Chemistry, Faculty of Science, Al-Balqa Applied University, Al-Salt 19117, Jordan. E-mail: khaleel.assaf@bau.edu.jo

^b Department of Chemistry, Faculty of Science, The Hashemite University, Zarqa 13133, Jordan. E-mail: fedaam@hu.edu.jo

^c Department of Chemistry, Faculty of Science, The University of Jordan, 11942 Amman, Jordan

† Electronic supplementary information (ESI) available: Additional spectral data. See DOI: <https://doi.org/10.1039/d4ya00620h>

selectivity for CC formation under mild and solvent/metal-free conditions.²⁹ Remarkably, ammonium-functionalized bis- β -CDs, synthesized by quaternizing the diamino-bridge with alkyl halides, efficiently catalyzed PC synthesis under 20 bar CO₂ pressure at 110 °C within 4 hours. Using 0.125 mol% catalyst, the turnover frequency (TOF) ranged from 71 to 198 h⁻¹, depending on the linker length and the identity of the nucleophile.³⁰ A calixarene-based cationic polymer was synthesized and utilized as a heterogeneous bifunctional catalyst for CC synthesis.²² Due to the accessible phenolic hydroxy groups on calixarene, which act as hydrogen bond donors, and the bromide anions on the linker serving as nucleophilic agents, excellent conversion and high selectivity were obtained under atmospheric CO₂ pressure using 1 mol% catalyst at 100 °C within 12 hours, without the need for a solvent or co-catalyst. It is noteworthy that host-guest interactions, one of the most prominent characteristics of macrocyclic compounds, have not been reported to play any role in the aforementioned catalysis.

Pillararenes, a class of macrocyclic molecules with a pillar-like structure, are composed of hydroquinone units linked by methylene bridges (**P5**, Scheme 1B). They can be easily functionalized in order to tailor their chemical properties.³¹ Guo *et al.* utilized **P5** to develop azo-bridged-based POPs as heterogeneous catalysts for the CO₂-epoxide coupling reaction. The catalysts showed excellent to good yields for different epoxides under mild conditions (80 °C, 1 MPa, 48 hours) in the presence of tetrabutylammonium bromide (TBAB) as a co-catalyst.³² The supramolecular complexation between amine-terminated **P5** and polyviologen was essential for ion separation, significantly enhancing the catalytic activity of the polyviologen compared to the free system, which exhibited very low yields.³³ Unlike the previous studies that employed **P5** as an auxiliary material, we present a novel catalytic approach exploiting the precise structure of trimethyl ammonium-rich pillar[5]arene (**N(Me)₃⁺-P5**, Scheme 1C) as a heterogeneous catalyst for CC synthesis. The catalyst was synthesized following the protocol reported by Huang and co-workers, which involved the cyclization of 1,4-bis(2-bromoethoxy)benzene with paraformaldehyde in the presence of boron trifluoride diethyl etherate. Subsequent treatment with excess trimethylamine produced **N(Me)₃⁺-P5**, featuring ten trimethylammonium groups on its upper and lower rims.³⁴ From a catalytic perspective, the catalyst design facilitates effective epoxide activation and nucleophilic ring-opening, while aiming to lower the required CO₂ pressure for the titled reaction. Specifically, the ammonium groups on both rims of **P5** offer multiple docking sites to activate the epoxide, while the bromide counter ions act as nucleophiles to promote the ring opening. In this study, all reactions were conducted using a CO₂ balloon. Epichlorohydrin (ECH) was used as a model compound to optimize the reaction conditions and evaluate the recyclability of the catalyst. The catalytic activity was further examined using a series of epoxides to assess its efficiency across different substrates. Additionally, density functional theory (DFT) calculations were performed to gain a deeper understanding of the reaction mechanism, specifically by evaluating the interaction energy between the catalyst, ECH and CO₂.

2. Experimental section

2.1. Materials

All chemicals were used without further purification. Ammonium-rich pillar[5]arene (**N(Me)₃⁺-P5**) was synthesized according to the literature.³⁴ The corresponding ¹H and ¹³C NMR spectra are provided in the ESI† (Fig. S1 and S2). Deuterium oxide (D₂O, 99.9% atom D), dimethyl sulfoxide-*d*₆ (DMSO-*d*₆, 99.5% atom D; kept over molecular sieve), epichlorohydrin (ECH, 99%), glycidol (GO, 96%), and 1,2-epoxy-3-phenoxypropane (EPOP, 99%) were obtained from Sigma-Aldrich. Styrene oxide (SO, 97%) and cyclohexene oxide (CHO, 98%) were from Acros Organics. Allyl glycidyl ether (AGE, >99%) was obtained from Thermo Fisher Scientific. Diethyl ether (98%) was received from LOBA chemie. CO₂ (99.95%, Food grade) and N₂ (industrial grade) were purchased from Advanced Technical Gases Co. (Amman, Jordan).

2.2. Instrumentation

¹H/¹³C nuclear magnetic resonance (NMR) spectra were measured using an AVANCE-III 400 MHz (¹H: 400 MHz, ¹³C: 100 MHz) equipped with a FTNMR Nano Bay spectrometer (Bruker, Switzerland).

2.3. Cyclic carbonate (CC) synthesis

The cycloaddition of CO₂ with epoxide was established with ECH as a model substrate. **N(Me)₃⁺-P5** (10 mg, 0.0044 mmol) was dispersed in 0.2 mL of DMSO-*d*₆ with continuous stirring for 30 minutes, followed by the addition of 0.05 mL ECH to the solution (0.7 mol% catalytic loading). Then, the reaction was carried out under CO₂ (balloon) at various reaction times and temperatures. The CC conversion was evaluated using ¹H NMR spectroscopy in DMSO-*d*₆.

2.4. Recyclability of the catalyst

The recyclability of **N(Me)₃⁺-P5** was investigated over five consecutive catalytic cycles using ECH as a substrate under the optimized reaction conditions (0.7 mol% catalyst, 80 °C and 8 hours). For each cycle, 15 mL of diethyl ether and 15 mL of ethanol were added to the reaction mixture to ensure complete precipitation of the catalyst and facilitate the separation. After 20 minutes, the clear reaction mixture was removed, and the process was repeated twice. The recovered catalyst was dried under nitrogen and reused by adding the same amount of ECH (0.05 mL).

2.5. Quantum-chemical calculations

Density functional theory (DFT) calculations were performed by using the Gaussian 16 software.³⁵ Geometry optimization and energy calculations (in DMSO, applying the implicit universal solvation model based on density, SMD³⁶) were performed with the B3LYP functional and Grimme's D3BJ dispersion correction method³⁷ along with the 6-31+G* basis set. The calculated interaction energy (ΔE) refers to energy difference between the molecular complex and the free components.

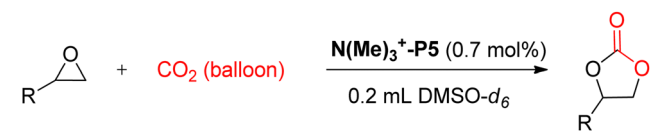


3. Results and discussion

3.1. Optimization of the reaction conditions

In this study, the catalyst design incorporates quaternary ammonium groups on both rims of the $\text{N}(\text{Me})_3^+\text{-P5}$ macrocycle, facilitating the activation of epoxide and CO_2 through ion-dipole interactions. The bromide counter anions act as nucleophiles to drive ring opening, eliminating the need for an external co-catalyst. The catalytic activity of $\text{N}(\text{Me})_3^+\text{-P5}$ was investigated using ECH as a model epoxide under ambient CO_2 pressure (balloon). Reactions were conducted at different temperatures and time intervals, with 0.7 mol% catalyst loading and 0.2 mL DMSO, as summarized in Table 1. The latter could be described as a green solvent for the catalytic reaction.³⁸ ECH was completely converted to 4-chloromethyl-2-oxo-1,3-dioxolane within 16 hours at 80 °C (Fig. S3, ESI[†]). Full conversion (>99%) was also observed within 12 hours at 80 °C (entry 1). Reducing the reaction time to 8 hours (entry 2) resulted in slightly lower conversions (90%), while further reduction to 4 hours led to a more significant drop (78%, entry 3). To optimize the temperature, additional experiments were conducted at 40 °C and room temperature (RT), both of which yielded significantly lower conversions (<15%) (entries 4 and 5). Thus, 80 °C was selected

Table 1 Cycloaddition reaction of CO_2 with ECH mediated by $\text{N}(\text{Me})_3^+\text{-P5}$ under different reaction times and temperatures (see Fig. S4–S8, ESI)



| Entry | Time/h | Temperature/°C | Conversion ^a /% |
|-------|--------|----------------|----------------------------|
| 1 | 12 | 80 | > 99 |
| 2 | 8 | 80 | 90 |
| 3 | 4 | 80 | 78 |
| 4 | 8 | 40 | 14 |
| 5 | 8 | RT | 12 |

^a Conversions were determined as an average of two trials and based on signal integration from the corresponding ^1H NMR spectra, with all reactions showing 100% selectivity.

as the optimal temperature for further experiments. Additionally, reducing the catalyst loading to 0.35 mol% still achieved high conversion (~90%, Fig. S9, ESI[†]) under the same conditions (80 °C and 8 hours), demonstrating a considerable turnover number (TON) of 290.

3.2. Conversion of various epoxides and catalyst reusability

To assess the general applicability of the $\text{N}(\text{Me})_3^+\text{-P5}$ catalyst, various epoxides (Fig. 1) were subjected to the cycloaddition reaction at 80 °C and 8 hours. Among the examined epoxides, glycidol (GO) showed excellent conversion (>97%) followed by ECH (90%). However, allyl glycidyl ether (AGE) exhibited a moderate conversion of 30%, and other substrates, such as internal and sterically hindered epoxides (cyclohexene oxide (CHO), styrene oxide (SO) and 2-epoxy-3-phenoxypropane (EPOP)), revealed very low conversions. Extending the reaction time up to 16 hours led to a notable improvement in the conversion of AGE to 85%, while the other epoxides showed minor enhancement (see ESI[†]). These findings suggest that the catalyst's performance is significantly influenced by the substrate steric factors (see DFT results).

$\text{N}(\text{Me})_3^+\text{-P5}$ is poorly soluble in the DMSO reaction mixture, due its macrocyclic structure and the ionic nature, which facilitates its separation for recyclability. After the reaction, the mixture was treated with diethyl ether and ethanol, followed by solvent removal and catalyst drying. $\text{N}(\text{Me})_3^+\text{-P5}$ showed excellent reusability for at least five consecutive cycles with ECH under the optimized reaction (Fig. 2), maintaining high conversion and selectivity.

3.3. Exploring reported multi-ammonium salts for epoxide- CO_2 coupling

Generally, multi-functionalized catalysts provide significant advantages over simpler structures, including enhanced catalytic activity, improved selectivity, and greater stability, making them highly attractive for complex and industrial-scale transformations. The performance of multi-ammonium scaffolds, employed for the chemical fixation of CO_2 with epoxides, has been compared to that of $\text{N}(\text{Me})_3^+\text{-P5}$, to highlight its effectiveness.

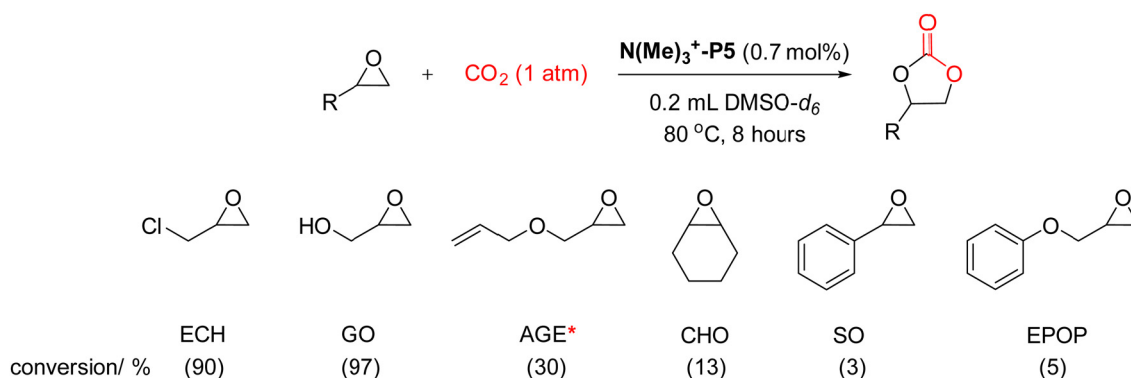


Fig. 1 The catalytic conversion of different epoxides by $\text{N}(\text{Me})_3^+\text{-P5}$. Conversions were determined through signal integration of the corresponding ^1H NMR spectra, with all reactions exhibiting 100% selectivity (see Fig. S10–S14, ESI[†]). *AGE achieved 85% conversion when the reaction time was extended to 16 hours (Fig. S15, ESI[†]).



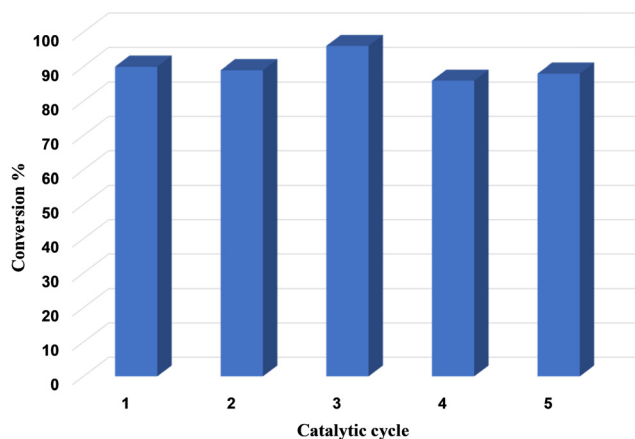


Fig. 2 Reusability of $\text{N}(\text{Me})_3^+\text{-P5}$ for multi-cycloaddition cycles using ECH as a substrate; see Fig. S19 (ESI[†]).

Theoretically, increasing the number of active sites within the catalyst is expected to enhance catalytic activity. However, this is not always the case. For instance, we reported a bifunctional phenolic-tri(ammonium) catalyst for the epoxide- CO_2 coupling reaction, where the large size of the bromide anion created a congested active site effect.³⁹ Interestingly, the non-congested version of the catalyst (entry 1, Table 2) exhibited higher catalytic activity compared to the multi-congested active site correspondent.³⁹ This highlights the importance of tuning catalytic activity by adjusting steric hindrance, which can be achieved through the use of appropriately designed spacers. Following a structural analogy to the previously discussed ammonium-functionalized bis- β -CDs,³⁰ quaternized 2,2',2'',2'''-(ethane-1,2-diylbis(azanetriyl))-tetrakis(ethan-1-ol) catalysts (entry 2, Table 2) demonstrated exceptional activity for PC synthesis. These catalysts achieved TOF values ranging from 112 to 133 h^{-1} under the optimized conditions.⁴⁰ Moving away from the multi-active site, bifunctionalized hydroxylated ammonium catalysts, a straightforward example involves the

use of supported quaternary ammonium salts. One such system is polyethylene glycol (PEG, $M_w = 6000$) covalently bound to tributylammonium bromide ($\text{PEG}(\text{NBu}_3\text{Br})_2$). This homogenous catalyst achieved 100% conversion in the selective synthesis of PC using only 0.5 mol% catalyst within 6 hours under supercritical conditions of 80 bar CO_2 pressure and 150 °C (entry 3, Table 2).⁴¹ Additionally, a series of deep eutectic solvent-modified lignins (entry 4, Table 2) were employed as heterogeneous catalysts for the reaction. These catalysts facilitated the synthesis of various CCs in high yields (90–99%) utilizing 100 mg of catalyst, 1 mmol of TBAB, and 10 bar of CO_2 . Notably, the catalysts demonstrated stability and reusability, retaining an 84% yield of glycidyl phenyl ether after five cycles.⁴²

Interestingly, beyond organocatalysts, incorporating four tetraalkylammonium bromide units in a bimetallic aluminium(salen) complex demonstrated high efficiency for converting terminal epoxides into CCs under ambient conditions at RT and atmospheric pressure (entry 5, Table 2).⁴³ Additionally, other multi-ammonium scaffolds, such as bifunctional borinane-based multi-ammonium salts, effectively catalyzed the ring-opening polymerization of PO, ECH and glycidyl azide with CO_2 .⁴⁴

3.4. Reaction mechanism and DFT calculations

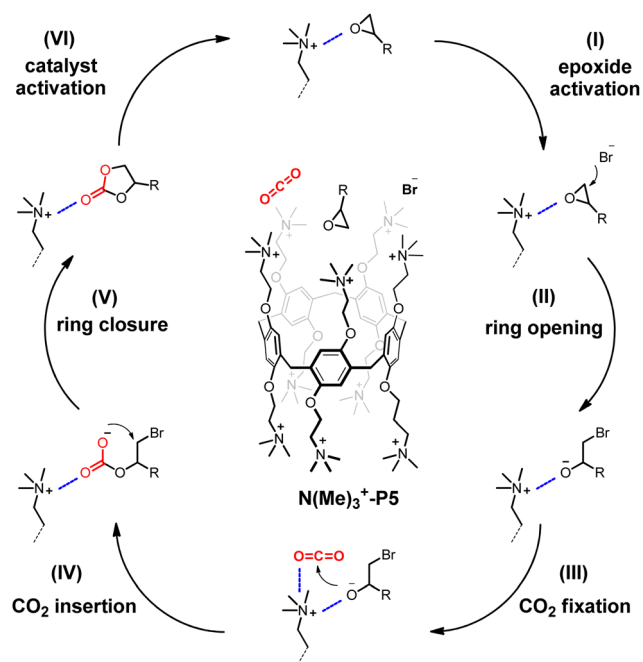
The postulated reaction mechanism for the coupling of CO_2 with epoxide in the presence of $\text{N}(\text{Me})_3^+\text{-P5}$ catalyst is shown in Scheme 2. Initially, the epoxide is associated with the catalyst through ion-dipole interactions between the epoxide's oxygen atom and the ammonium groups on $\text{N}(\text{Me})_3^+\text{-P5}$, which leads to the polarization of the C–O bond of the epoxide. This is followed by the ring opening step, in which the nucleophilic bromide anion attacks the epoxide from the less hindered carbon atom to form an alkoxide intermediate. Then, the anionic oxygen atom reacts with the electrophilic CO_2 , which is also activated through ion-dipole interactions, to form the carbonate adduct. Subsequently, CC is produced upon intramolecular ring closure, simultaneously regenerating the catalyst.

Table 2 Different catalytic systems including multi-ammonium salts reported in the literature compared with $\text{N}(\text{Me})_3^+\text{-P5}$ for the cycloaddition reaction of ECH and CO_2

| Entry | Catalyst | Catalyst loading/mol% | Time/h | CO_2 pressure/bar | Temperature/°C | Conversion, yield/% | Ref. |
|-------|-------------------------------------|-----------------------|--------|----------------------------|----------------|---------------------|-----------|
| 1 | Cat1 | 2 | 24 | 1 | 90 | > 99 | 39 |
| 2 | Cat2 | 0.25 | 3 | 20 | 120 | 97 | 40 |
| 3 | Cat3 | 0.5 | 6 | 50 | 120 | 92 | 41 |
| 4 | Cat4 | — ^a | 3 | 10 | 110 | 98 | 42 |
| 5 | Cat5 | 2.5 | 6 | 1 | 25 | 100 | 43 |
| 6 | $\text{N}(\text{Me})_3^+\text{-P5}$ | 0.7 | 12 | 1 | 80 | > 99 | This work |

^a The 100 mg catalyst loading was used in the presence of 1 mmol TBAB.





Scheme 2 Proposed catalytic reaction mechanism of the cycloaddition reaction between CO_2 and epoxides by $\text{N}(\text{Me})_3^+\text{-P5}$.

To elucidate the mechanism of the cycloaddition reaction, DFT calculations were performed to investigate the interaction between the $\text{N}(\text{Me})_3^+\text{-P5}$ and the reactants (ECH and CO_2) in DMSO. It should be noted that due to the limited solubility of $\text{N}(\text{Me})_3^+\text{-P5}$ in DMSO, the interaction mode could not be explored experimentally. Fig. 3A shows the optimized structure of $\text{N}(\text{Me})_3^+\text{-P5}$, which indicated that the trimethyl ammonium groups are uniformly distributed around the upper and lower rims of the macrocyclic framework, making them accessible to establish intermolecular interactions with the reactants. The

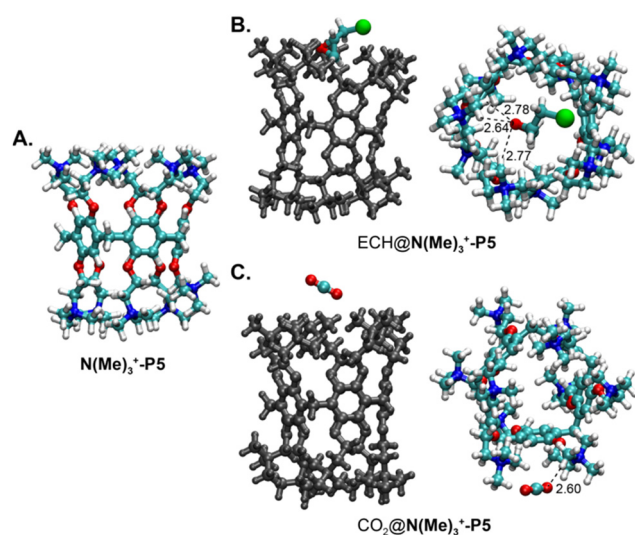


Fig. 3 DFT-optimized structure (B3LYP-D3/6-31+G*, in DMSO) of (A) free $\text{N}(\text{Me})_3^+\text{-P5}$, (B) the $\text{ECH@N}(\text{Me})_3^+\text{-P5}$ complex, and (C) the $\text{CO}_2@N(\text{Me})_3^+\text{-P5}$ complex.

DFT results indicated that ECH formed strong ion-dipole interactions with ammonium groups of the catalyst as revealed by the short intermolecular interaction distances (Fig. 3B) and calculated interaction energy (ΔE) of $-7.8 \text{ kcal mol}^{-1}$. It was also observed that the substituent on the epoxide (for example, $-\text{CH}_2\text{Cl}$ for ECH) is positioned outside the macrocyclic structure. This orientation might explain the low reactivity of the sterically hindered epoxides, in which the large substituent (as in the case of SO and EPOP) acts as a shield making the nucleophilic ring opening less accessible. CO_2 binds with $\text{N}(\text{Me})_3^+\text{-P5}$ through electrostatic interaction with a ΔE value of $-3.8 \text{ kcal mol}^{-1}$ (Fig. 3C). These findings suggest the dual interaction capability of the catalyst with reactants facilitates ECH activation and direct CO_2 molecules for the subsequent step. The counter anion (Br^-) promotes the ring-opening step required for CC synthesis. These results highlight the multifunctional nature of $\text{N}(\text{Me})_3^+\text{-P5}$ in catalyzing the reaction through synergistic interactions with both reactants.

4. Conclusions

In summary, a trimethyl ammonium-rich pillar[5]arene macrocycle is used as a heterogeneous organocatalyst for the cycloaddition of CO_2 with epoxides, enabling the generation of cyclic carbonates under ambient conditions. The catalyst functions without the need for a co-catalyst, which is a prerequisite for other macrocyclic molecules,^{28,45} and could be recycled several times without affecting the catalytic performance.

Author contributions

K. I. A. writing – original draft, methodology, investigation, conceptualization. F. M. Q. writing – review & editing, methodology, investigation, supervision, conceptualization. A. F. E. writing – review & editing, methodology, investigation. A. K. Q. writing – review & editing, methodology, investigation. A. M. A. data curation, formal analysis, investigation. M. M. A. data curation, formal analysis, investigation.

Data availability

The data supporting this article have been included as part of the ESI.†

Conflicts of interest

The authors declare no competing financial interest.

Acknowledgements

F. M. Q. acknowledges the Deanship of Scientific Research at the Hashemite University for financial support (grant number: 88/2023).



References

- 1 Y. Chen and T. Mu, *Green Chem.*, 2019, **21**, 2544–2574.
- 2 Y. Wang, W. Gao, S. Kazumi, H. Li, G. Yang and N. Tsubaki, *Chem. – Eur. J.*, 2019, **25**, 5149–5153.
- 3 A. K. Qaroush, A. a F. Eftaiha, A. H. Smadi, K. I. Assaf, F. a M. Al-Qaisi and F. Alsoubani, *ACS Omega*, 2022, **7**, 22511–22521.
- 4 T. Yan, H. Liu, Z. X. Zeng and W. G. Pan, *J. CO₂ Util.*, 2023, **68**, 102355.
- 5 P. P. Pescarmona, *Curr. Opin. Green Sustainable Chem.*, 2021, **29**, 100457.
- 6 J. H. Clements, *Ind. Eng. Chem. Res.*, 2003, **42**, 663–674.
- 7 A. Rehman, F. Saleem, F. Javed, A. Ikhtlaq, S. W. Ahmad and A. Harvey, *J. Environ. Chem. Eng.*, 2021, **9**, 105113.
- 8 A. K. Qaroush, A. K. Hasan, S. B. Hammad, F. A. M. Al-Qaisi, K. I. Assaf, F. Alsoubani and A. A. F. Eftaiha, *New J. Chem.*, 2021, **45**, 22280–22288.
- 9 P. Anastas and N. Eghbali, *Chem. Soc. Rev.*, 2010, **39**, 301–312.
- 10 V. Caló, A. Nacci, A. Monopoli and A. Fanizzi, *Org. Lett.*, 2002, **4**, 2561–2563.
- 11 T. Ema, K. Fukuhara, T. Sakai, M. Ohbo, F.-Q. Bai and J.-Y. Hasegawa, *Catal. Sci. Technol.*, 2015, **5**, 2314–2321.
- 12 S. Ghazali-Esfahani, H. Song, E. Păunescu, F. D. Bobbink, H. Liu, Z. Fei, G. Laurenczy, M. Bagherzadeh, N. Yan and P. J. Dyson, *Green Chem.*, 2013, **15**, 1584–1589.
- 13 O. Martínez-Ferraté, G. Chacón, F. Bernardi, T. Grehl, P. Brüner and J. Dupont, *Catal. Sci. Technol.*, 2018, **8**, 3081–3089.
- 14 A. Belinchón, Á. Pereira, E. Hernández, P. Navarro and J. Palomar, *J. CO₂ Util.*, 2024, **85**, 102886.
- 15 V. D'Elia, J. D. A. Pelletier and J.-M. Basset, *ChemCatChem*, 2015, **7**, 1906–1917.
- 16 F. a M. Al-Qaisi, A. K. Qaroush, K. I. Assaf, A. a F. Eftaiha, I. K. Okashah, A. H. Smadi, F. Alsoubani, A. S. Barham and T. Repo, *Inorg. Chim. Acta*, 2023, **557**, 121716.
- 17 F. a M. Al-Qaisi, A. K. Qaroush, A. H. Smadi, F. Alsoubani, K. I. Assaf, T. Repo and A. a F. Eftaiha, *Dalton Trans.*, 2020, **49**, 7673–7679.
- 18 T. K. Pal, D. De and P. K. Bharadwaj, *Coord. Chem. Rev.*, 2020, **408**, 213173.
- 19 R. Babu, A. C. Kathalikkattil, R. Roshan, J. Tharun, D.-W. Kim and D.-W. Park, *Green Chem.*, 2016, **18**, 232–242.
- 20 R. Luo, Y. Yang, K. Chen, X. Liu, M. Chen, W. Xu, B. Liu, H. Ji and Y. Fang, *J. Mater. Chem. A*, 2021, **9**, 20941–20956.
- 21 R. Luo, M. Chen, X. Liu, W. Xu, J. Li, B. Liu and Y. Fang, *J. Mater. Chem. A*, 2020, **8**, 18408–18424.
- 22 Y. Zhang, K. Su, Z. Hong, Z. Han and D. Yuan, *Ind. Eng. Chem. Res.*, 2020, **59**, 7247–7254.
- 23 Y. Xie, T.-T. Wang, X.-H. Liu, K. Zou and W.-Q. Deng, *Nat. Commun.*, 2013, **4**, 1960.
- 24 M. E. Davis and M. E. Brewster, *Nat. Rev. Drug Discovery*, 2004, **3**, 1023–1035.
- 25 K. I. Assaf and W. M. Nau, *Chem. Soc. Rev.*, 2015, **44**, 394–418.
- 26 V. Böhmer, *Angew. Chem., Int. Ed. Engl.*, 1995, **34**, 713–745.
- 27 M. Xue, Y. Yang, X. Chi, Z. Zhang and F. Huang, *Acc. Chem. Res.*, 2012, **45**, 1294–1308.
- 28 J. Song, Z. Zhang, B. Han, S. Hu, W. Li and Y. Xie, *Green Chem.*, 2008, **10**, 1337–1341.
- 29 Q. Wen, X. Yuan, Q. Zhou, H. J. Yang, Q. Jiang, J. Hu and C. Y. Guo, *Materials*, 2023, **16**, 53.
- 30 J. Peng, S. Wang, H.-J. Yang, B. Ban, Z. Wei, L. Wang and L. Bo, *Catal. Today*, 2019, **330**, 76–84.
- 31 N. L. Strutt, H. Zhang, S. T. Schneebeli and J. F. Stoddart, *Acc. Chem. Res.*, 2014, **47**, 2631–2642.
- 32 Q. Guo, S. Zhang and W. Gong, *J. Polym. Sci.*, 2024, **62**, 1664–1672.
- 33 Y. Zhou, Z. Liu, Z. Yang, Y. Zheng, M. Yang, W. Feng, X. Li and L. Yuan, *Chem. Commun.*, 2024, **60**, 300–303.
- 34 Y. Ma, X. Ji, F. Xiang, X. Chi, C. Han, J. He, Z. Abliz, W. Chen and F. Huang, *Chem. Commun.*, 2011, **47**, 12340–12342.
- 35 M. J. Frisch, H. B. Schlegel, G. E. Scuseria, M. A. Robb, J. R. Cheeseman, G. Scalmani, V. Barone, G. A. Petersson, H. Nakatsuji, X. Li, M. Caricato, A. V. Marenich, J. Bloino, B. G. Janesko, R. Gomperts, B. Mennucci, H. P. Hratchian, J. V. Ortiz, A. F. Izmaylov, J. L. Sonnenberg, D. Williams-Young, F. Ding, F. Lipparini, F. Egidi, J. Goings, B. Peng, A. Petrone, T. Henderson, D. Ranasinghe, V. G. Zakrzewski, J. Gao, N. Rega, G. Zheng, W. Liang, M. Hada, M. Ehara, K. Toyota, R. Fukuda, J. Hasegawa, M. Ishida, T. Nakajima, Y. Honda, O. Kitao, H. Nakai, T. Vreven, K. Throssell, J. A. Montgomery Jr, J. E. Peralta, F. Ogliaro, M. J. Bearpark, J. J. Heyd, E. N. Brothers, K. N. Kudin, V. N. Staroverov, T. A. Keith, R. Kobayashi, J. Normand, K. Raghavachari, A. P. Rendell, J. C. Burant, S. S. Iyengar, J. Tomasi, M. Cossi, J. M. Millam, M. Klene, C. Adamo, R. Cammi, J. W. Ochterski, R. L. Martin, K. Morokuma, O. Farkas, J. B. Foresman and D. J. Fox, *Gaussian 16*, Gaussian, Inc., Wallingford CT, 2016.
- 36 A. V. Marenich, C. J. Cramer and D. G. Truhlar, *J. Phys. Chem. B*, 2009, **113**, 6378–6396.
- 37 S. Grimme, S. Ehrlich and L. Goerigk, *J. Comput. Chem.*, 2011, **32**, 1456–1465.
- 38 A. K. Qaroush, K. I. Assaf, S. K. Bardaweel, A. A. Al-Khateeb, F. Alsoubani, E. Al-Ramahi, M. Masri, T. Brück, C. Troll, B. Rieger and A. A. F. Eftaiha, *Green Chem.*, 2017, **19**, 4305–4314.
- 39 M. H. Al-Anati, A. K. Qaroush, A. A. F. Eftaiha, S. B. Hammad, F. A. M. Al-Qaisi and K. I. Assaf, *New J. Chem.*, 2024, **48**, 19750–19762.
- 40 J. Peng, S. Wang, H.-J. Yang, B. Ban, Z. Wei, L. Wang and B. Lei, *Fuel*, 2018, **224**, 481–488.
- 41 Y. Du, J.-Q. Wang, J.-Y. Chen, F. Cai, J.-S. Tian, D.-L. Kong and L.-N. He, *Tetrahedron Lett.*, 2006, **47**, 1271–1275.
- 42 X. Xiong, H. Zhang, S. L. Lai, J. Gao and L. Gao, *React. Funct. Polym.*, 2020, **149**, 104502.
- 43 J. Meléndez, M. North and P. Villuendas, *Chem. Commun.*, 2009, 2577–2579.
- 44 V. K. Chidara, Y. Gnanou and X. Feng, *Polym. Chem.*, 2024, **15**, 2492–2501.
- 45 S. Wang, J. Peng, H.-J. Yang, B. Ban, L. Wang, B. Lei, C.-Y. Guo, J. Hu, J. Zhu and B. Han, *J. Nanosci. Nanotechnol.*, 2019, **19**, 3263–3268.

